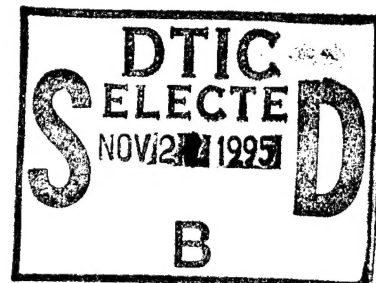


**PL-TR-95-2133**

**ANALYZE DATA FROM THE PASP PLUS DOSIMETER  
ON THE APEX SPACECRAFT**

**Frederick A. Hanser  
Paul R. Morel**

**PANAMETRICS, INC.  
221 Crescent Street  
Waltham, MA 02154-3497**



**22 September 1995**

**Scientific Report No. 1**

**Approved for Public Release; Distribution Unlimited**

**DTIC QUALITY INSPECTED 6**



**PHILLIPS LABORATORY  
Directorate of Geophysics  
AIR FORCE MATERIEL COMMAND  
HANSCOM AFB, MA 01731-3010**

**19951120 092**

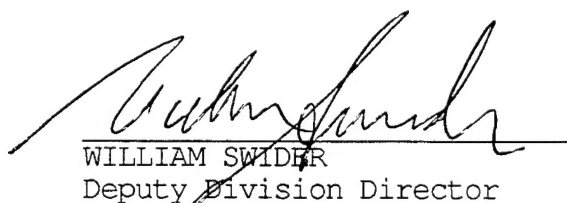
This technical report has been reviewed and is approved for publication.



DONALD A. GUIDICE  
Contract Manager



DAVID A. HARDY  
Branch Chief



WILLIAM SWIDER  
Deputy Division Director

This report has been reviewed by the ESC Public Affairs Office (PA) and is releasable to the National Technical Information Service (NTIS).

Qualified requestors may obtain additional copies from the Defense Technical Information Center (DTIC). All others should apply to the National Technical Information Service (NTIS).

If your address has changed, or if you wish to be removed from the mailing list, or if the addressee is no longer employed by your organization, please notify PL/IM, 29 Randolph Road, Hanscom AFB, MA 01731-3010. This will assist us in maintaining a current mailing list.

Do not return copies of this report unless contractual obligations or notices on a specific document requires that it be returned.

# REPORT DOCUMENTATION PAGE

*Form Approved  
OMB No. 0704-0188*

Public reporting burden for this collection of information is estimated to average 1 hour per response, including the time for reviewing instructions, searching existing data sources, gathering and maintaining the data needed, and completing and reviewing the collection of information. Send comments regarding this burden estimate or any other aspect of this collection of information, including suggestions for reducing this burden, to Washington Headquarters Services, Directorate for Information Operations and Reports, 1215 Jefferson Davis Highway, Suite 1204, Arlington, VA 22202-4302, and to the Office of Management and Budget, Paperwork Reduction Project (0704-0188), Washington, DC 20503.

1. AGENCY USE ONLY (Leave blank)			2. REPORT DATE 22 September 1995	3. REPORT TYPE AND DATES COVERED Scientific No. 1	
4. TITLE AND SUBTITLE Analyze Data from the PASP Plus Dosimeter on the APEX Spacecraft			5. FUNDING NUMBERS Contract Number: F19628-93-C-0151 PE 63410F PR 2822 TA GC WUPN		
6. AUTHOR(S) Frederick A. Hanser, Paul R. Morel			8. PERFORMING ORGANIZATION REPORT NUMBER		
7. PERFORMING ORGANIZATION NAME(S) AND ADDRESS(ES) Panametrics, Inc. 221 Crescent Street Waltham, MA 02154-3497			10. SPONSORING / MONITORING AGENCY REPORT NUMBER PL-TR-95-2133		
9. SPONSORING / MONITORING AGENCY NAME(S) AND ADDRESS(ES) Phillips Laboratory 29 Randolph Road Hanscom AFB, MA 01731-3010  Contract Monitor: Donald Guidice/GPSG			11. SUPPLEMENTARY NOTES		
12a. DISTRIBUTION / AVAILABILITY STATEMENT Approved for public release; Distribution unlimited.			12b. DISTRIBUTION CODE		
13. ABSTRACT (Maximum 200 words) Data analysis procedures for the PASP Plus Dosimeter have been specified, and the calibration constants for the SN/2 unit in the APEX spacecraft have been provided. The SN/1 unit calibration data from the MIT Van de Graaff have been reduced to geometric factors. The new calibrated geometric factors for the 1 MeV electron threshold D2A and D2B detectors deviate slightly from the earlier calibrations of the CRRES Dosimeter 1 MeV electron threshold D1 detector. The PASP Plus Dosimeter electron calibration data are believed to be the more accurate, and are likely to apply to the CRRES D1 detector.					
14. SUBJECT TERMS Dosimeter Electron Flux			15. NUMBER OF PAGES 28		
16. PRICE CODE			17. SECURITY CLASSIFICATION OF REPORT UNCLASSIFIED		
18. SECURITY CLASSIFICATION OF THIS PAGE UNCLASSIFIED			19. SECURITY CLASSIFICATION OF ABSTRACT UNCLASSIFIED		
20. LIMITATION OF ABSTRACT UNLIMITED					

## Table of Contents

1. Introduction	1
2. PASP Plus Dosimeter Design and Data Reduction	1
2.1 Summary of Dosimeter Design and Operation	1
2.2 General Method for Data Analysis	2
3. Calibration with Electrons at a Van de Graaff Accelerator	5
3.1 Set-up and Data Analysis Method	5
3.2 Calibrated Electron Response	12
4. Summary and Conclusions	19
References	21

Accession For	
NTIS GRA&I	<input checked="" type="checkbox"/>
DTIC TAB	<input type="checkbox"/>
Unannounced	<input type="checkbox"/>
Justification	
By _____	
Distribution/	
Availability Codes	
Dist	Avail and/or Special
A-1	

## List of Figures

<u>Figure</u>		<u>Page</u>
1	Isometric View of the PASP Plus Dosimeter	2
2	PASP Plus Dosimeter Electronics Block Diagram	3
3	Experimental Configuration for Electron Calibration at the MIT Van de Graaff	7
4	Electronics and Control Configuration for Electron Calibration at the MIT Van de Graaff	8
5	Electron Energy Calibration of the MIT Van de Graaff	11
6	Dosimeter SN/1 D1A Calibrated Electron Geometric Factors	14
7	Dosimeter SN/1 D1B Calibrated Electron Geometric Factors	15
8	Dosimeter SN/1 D2A Calibrated Electron Geometric Factors	16
9	Dosimeter SN/1 D2B Calibrated Electron Geometric Factors	17
10	Dosimeter SN/1 D3 Calibrated Electron Geometric Factors	18
11	Measured Angular Response of D1B for Electrons	20
12	Measured Angular Response of D2B for Electrons	20

## List of Tables

<u>Table</u>		<u>Page</u>
1	Summary of PASP Plus Dosimeter SN/2 Dome and Detector Properties	4
2	PASP Plus Dosimeter Particle Energy Detection Ranges	4
3	Primary Science Data Entities	5
4	PASP Plus Dosimeter SN/2 Dose Channel Calibration Factors	6
5	PASP Plus Dosimeter SN/2 In-Flight Calibration Source Count Rates	6
6	Summary of PASP Plus Dosimeter SN/1 Calibration Run Sets	9
7	Electron Energy Calibration for Dosimeter SN/1 Calibration	10
8	Dosimeter SN/1 D1A and D1B Calibrated Electron Responses	13
9	Dosimeter SN/1 D2A and D2B Calibrated Electron Responses	13
10	Dosimeter SN/1 D3 Calibrated Electron Responses	18

## 1. Introduction

The Advanced Photovoltaic and Electronic Experiments (APEX) satellite carries the Photovoltaic Array Space Power Plus Diagnostics (PASP Plus) experiment. PASP Plus includes a Dosimeter to provide a measurement of the particle doses and fluxes behind four thicknesses of aluminum shielding. The PASP Plus Dosimeter design and calibration are described in Reference 1. Two Dosimeters were fabricated to provide a flight unit and a backup unit. Dosimeter SN/2 is on the APEX spacecraft, which was launched on 3 August 1994.

A general discussion of the Dosimeter design and data reduction procedures is given in Section 2. More detailed information on the design is given in Reference 1, and it is expected that data analysis procedures will be modified as actual in-orbit data become available. Section 3 contains the results of electron calibration of the SN/1 Dosimeter at a Van de Graaff accelerator. The accelerator only provided electron beams up to about 3.5 MeV, which allowed detailed calibration of only the two thinnest aluminum shields.

## 2. PASP Plus Dosimeter Design and Data Reduction

### 2.1 Summary of Dosimeter Design and Operation

The PASP Plus Dosimeter design and operation are described in detail in Reference 1. The dosimeter contains six solid state detectors (SSDs) behind four thicknesses (domes) of aluminum (Al) shielding. The two thinnest Al shields have two SSDs of different areas to allow for a wider dynamic range in incident particle flux. The thinnest dome (D1) is a flat shield of 4.3 mil thick Al, while the other three domes (D2, D3 and D4) are Al hemispheres. The SSDs are shielded from rear entry particles by a 0.5 inch thick tungsten shield, so they have an approximately  $2\pi$  sr FOV. A weak Am-241 calibration source is located behind each SSD to provide a check on SSD gain and total depletion. An isometric view of the Dosimeter is given in Figure 1, and a block diagram of the electronics is shown in Figure 2.

The Dosimeter SN/2 is in the APEX PASP Plus payload, with its dome and detector properties being summarized in Table 1. The nominal particle detection energy ranges are summarized in Table 2, and are based on nominal range-energy table calculations. The high energy proton shift from HILET to LOLET is an average of the  $0^\circ$  and  $60^\circ$  energies for D1, and is the  $60^\circ$  energy for D2, D3 and D4. Detailed energy loss curves for the four domes are given in Reference 1. The VHILET energy losses are also given in Table 1, with the count data providing a measure of the proton nuclear "star" production, which is associated with SEUs in sensitive electronic devices.

The output data stream provides a set of flux counts and integrated dose counts for the LOLET and HILET channels, and a number of additional counts as listed in Table 3. Normal output

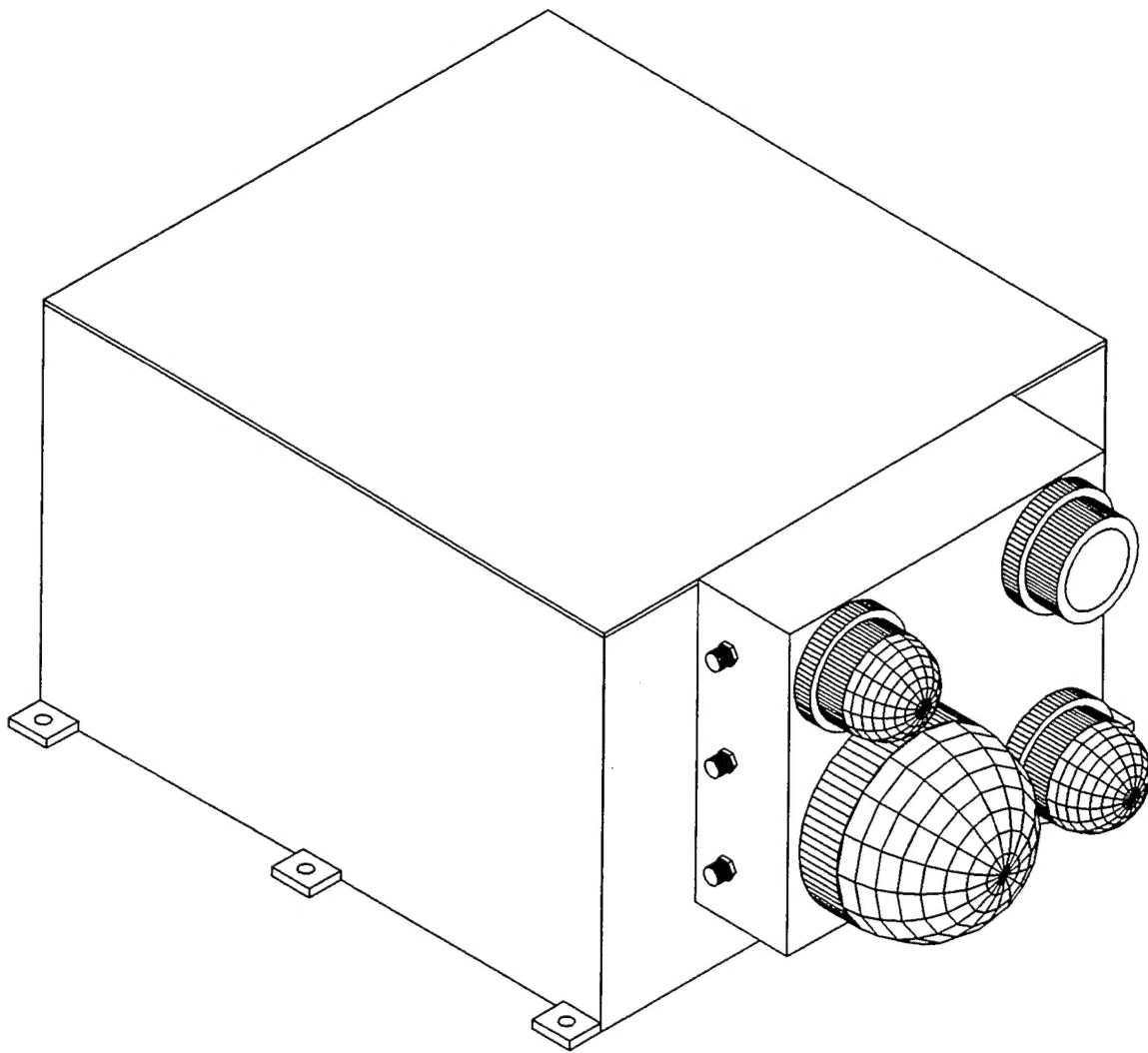


Figure 1. Isometric View of the PASP Plus Dosimeter.

provides a set of data for one channel every second, with a complete set for all six channels being obtained every 6 seconds. Details of the command and telemetry operation and formats are given in Reference 1.

## 2.2 General Method for Data Analysis

The dosimeter doses are accumulated continuously from turn-on, unless they are reset by command. The accumulated total doses, LOLET and HILET, are calculated from the telemetered data using the dose calibration constants in Table 4. Since the complete dose counts are output, dose rates can be calculated by taking the difference of successive (6 sec interval) dose counts.

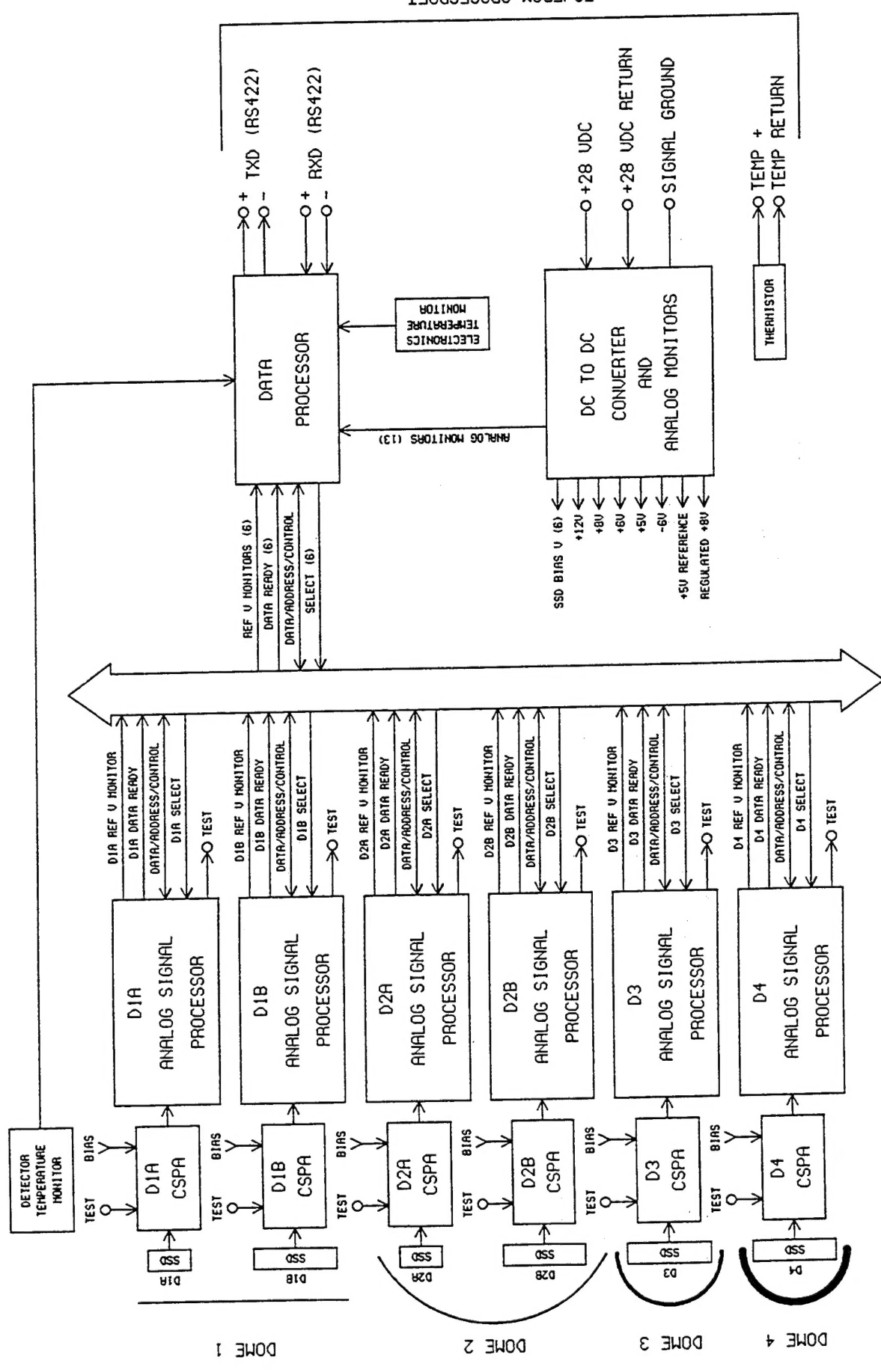


Figure 2. PASP Plus Dosimeter Electronics Block Diagram.

Table 1: Summary of PASP Plus Dosimeter SN/2 Dome and Detector Properties

Dome and Detector No.	Aluminum Shield		Detector		VHILET E Loss (MeV)
	(mils)	(g/cm <sup>2</sup> )	Area (A <sub>no</sub> ) (cm <sup>2</sup> )	Thickness (microns)	
D1/D1A	4.29	0.0294	0.00815	416	40
D1/D1B	4.29	0.0294	0.0514	393	40
D2/D2A	82.5	0.57	0.00815	417	40
D2/D2B	82.5	0.57	0.0514	382	40
D3	232.5	1.59	0.0514	400	40
D4	457.5	3.14	1.000	396	75

Table 2: PASP Plus Dosimeter Particle Energy Detection Ranges

Dome No.	LOLET Particles		HILET Protons (MeV)	VHILET Protons (MeV)
	Electrons (T <sub>n</sub> ) (MeV)	Protons (MeV)		
D1	>0.15	>80	5 - 80	>40
D2	>1.0	>115	20 - 115	>46
D3	>2.5	>120	32 - 120	>56
D4	>5.0	>125	52 - 125	>95

Flux counts can be used with the calibrated geometric factors to provide particle flux data. The flux counts are reset after each readout, so they correspond to 6 s accumulation times. Under conditions of low ambient particle fluxes, the HILETA and HILETB counts can be used to verify SSD gain and total depletion by comparison with the pre-launch calibration source counts. The dosimeter SN/2 calibration source count rates for all channels are listed in Table 5. For periods of low ambient fluxes, the measured dose and flux counts must be corrected for the calibration source count rates to provide true ambient particle dose and flux measurements.

The electron response of the LOLET flux channels for previous dosimeters with identical dome designs was calibrated at accelerators and summarized in References 2 and 3. The energy dependent electron geometric factors for dome n, in cm<sup>2</sup>-sr, are given by the equation

$$\begin{aligned}
 G_{fen}(E) &= 0 & E/T_n &< 1 \\
 &= 7.38 \times A_{no} \times (1 - T_n/E) & 1 \leq E/T_n \leq 3 & (2.1) \\
 &= 4.92 \times A_{no} & E/T_n &\geq 3
 \end{aligned}$$

with  $A_{no}$  being the SSD area from Table 1 and  $T_n$  being the electron threshold energy from Table 2. The proton geometric factors are to first order given by  $\pi \times A_{no}$  cm<sup>2</sup>-sr, with  $A_{no}$  being the SSD area of Table 1. The proton energy responses vary with the angle of incidence because of the change in path length in the SSD sensitive volume, so the ranges in Table 2 are approximate averages, as are the nominal geometric factors.

The electron calibration data for the PASP Plus dosimeter SN/1 given in Section 3 are at variance with the form of Eq. (2.1), especially the effective electron threshold energy, so the lower energy electron calibrations for the previous dosimeters are questionable. This affects only the electron flux calculations, and has no effect on the dose calibrations. A more detailed discussion is given in Section 3.

Table 3: Primary Science Data Entities

Entity	Mnemonic
Processed 50 keV to 1 MeV Event Count	LOLET COUNT
Processed 1 MeV to 3 Mev Event Count	HILETA COUNT
Processed 3 Mev to 10 MeV Event Count	HILETB COUNT
Processed Digital to Analog Converter Overflow Event Count ( $\geq 10$ MeV)	OVERFLOW COUNT
Very High Energy Deposition Event Count ( $\geq 40$ MeV for D1A, D1B, D2A, D2B and D3) ( $\geq 75$ MeV for D4)	VHILET COUNT
Total Event Count ( $\geq 50$ keV)	TOTAL COUNT
50 keV to 1 MeV Dose	LOLET DOSE
1 MeV to 10 MeV Dose	HILET DOSE

### 3. Calibration with Electrons at a Van de Graaff Accelerator

#### 3.1 Set-up and Data Analysis Method

The geometry of the calibration set-up at the MIT Van de Graaff is shown in Figure 3. The Dosimeter SN/1 was positioned on a rotating table 25 inches from the exit window of the 90° analyzing magnet vacuum pipe, with two monitor detectors M1 and M2 positioned as shown. The monitor detectors had precise collimators to measure the true electron beam intensity. Since the monitors

Table 4: PASP Plus Dosimeter SN/2 Dose Channel Calibration Factors

SSD	Area (cm <sup>2</sup> )	Thickness (microns)	LOLET Dose Calibration				HILET Dose Calibration			
			keV		Gray		keV		Gray	
			Digitizer count	TM dose count	TM dose count	Gray	Digitizer count	TM dose count	rad	rad
D1A	0.00815	416	37.3	7.57x10 <sup>-7</sup>	7.57x10 <sup>-9</sup>	38.3	6.21x10 <sup>-6</sup>	6.21x10 <sup>-8</sup>		
D1B	0.0514	393	38.4	1.306x10 <sup>-7</sup>	1.306x10 <sup>-9</sup>	39.2	1.067x10 <sup>-6</sup>	1.067x10 <sup>-8</sup>		
D2A	0.00815	417	38.7	7.83x10 <sup>-7</sup>	7.83x10 <sup>-9</sup>	39.8	6.44x10 <sup>-6</sup>	6.44x10 <sup>-8</sup>		
D2B	0.0514	382	39.1	1.369x10 <sup>-7</sup>	1.369x10 <sup>-9</sup>	40.1	1.123x10 <sup>-6</sup>	1.123x10 <sup>-8</sup>		
D3	0.0514	400	37.6	1.257x10 <sup>-7</sup>	1.257x10 <sup>-9</sup>	39.1	1.045x10 <sup>-6</sup>	1.045x10 <sup>-8</sup>		
D4	1.000	396	39.2	6.81x10 <sup>-9</sup>	6.81x10 <sup>-11</sup>	40.6	5.64x10 <sup>-6</sup>	5.64x10 <sup>-10</sup>		

Table 5: PASP Plus Dosimeter SN/2 In-Flight Calibration Source Count Rates

SSD	LOLET Count Rates (cps)		HILET Count Rates (cps)				Telemetered Dose*
	Flux	Dose	HILETB Flux	HILETB	HILETA	Actual Dose	
D1A	0.091	0.778	0.137	0.250	0.548	30.4	3.80
D1B	0.170	2.045	0.487	0.639	0.762	84.0	10.51
D2A	0.054	0.459	0.082	0.150	0.543	18.1	2.26
D2B	0.159	1.772	0.802	0.633	1.266	100.6	12.57
D3	0.087	0.854	0.352	0.591	0.596	72.8	9.10
D4	0.259	2.024	0.759	0.954	0.796	127.4	15.94

\* HILET Telemetered Dose = 1/8 HILET Actual Dose

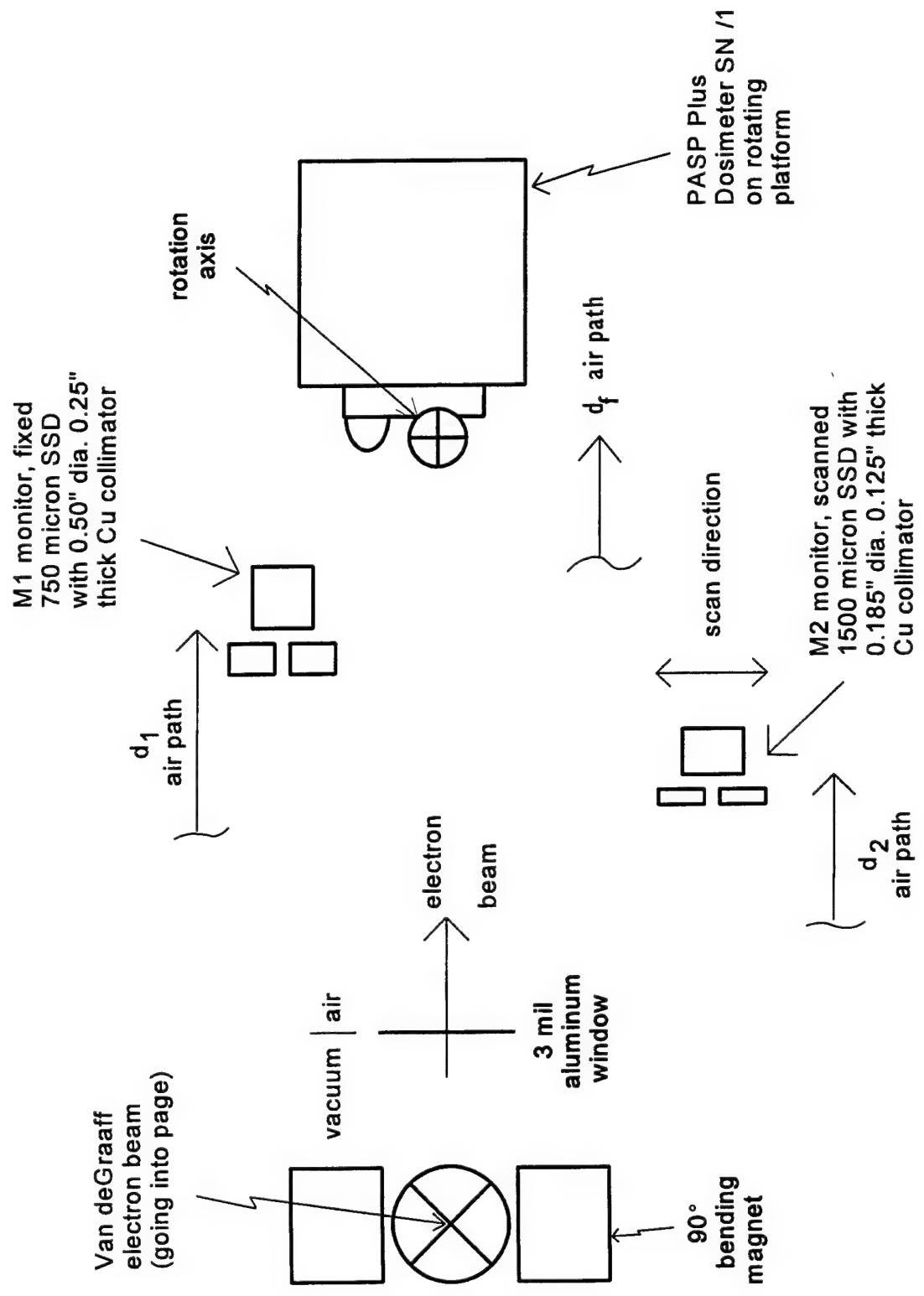


Figure 3. Experimental Configuration for Electron Calibration at the MIT Van de Graaff.

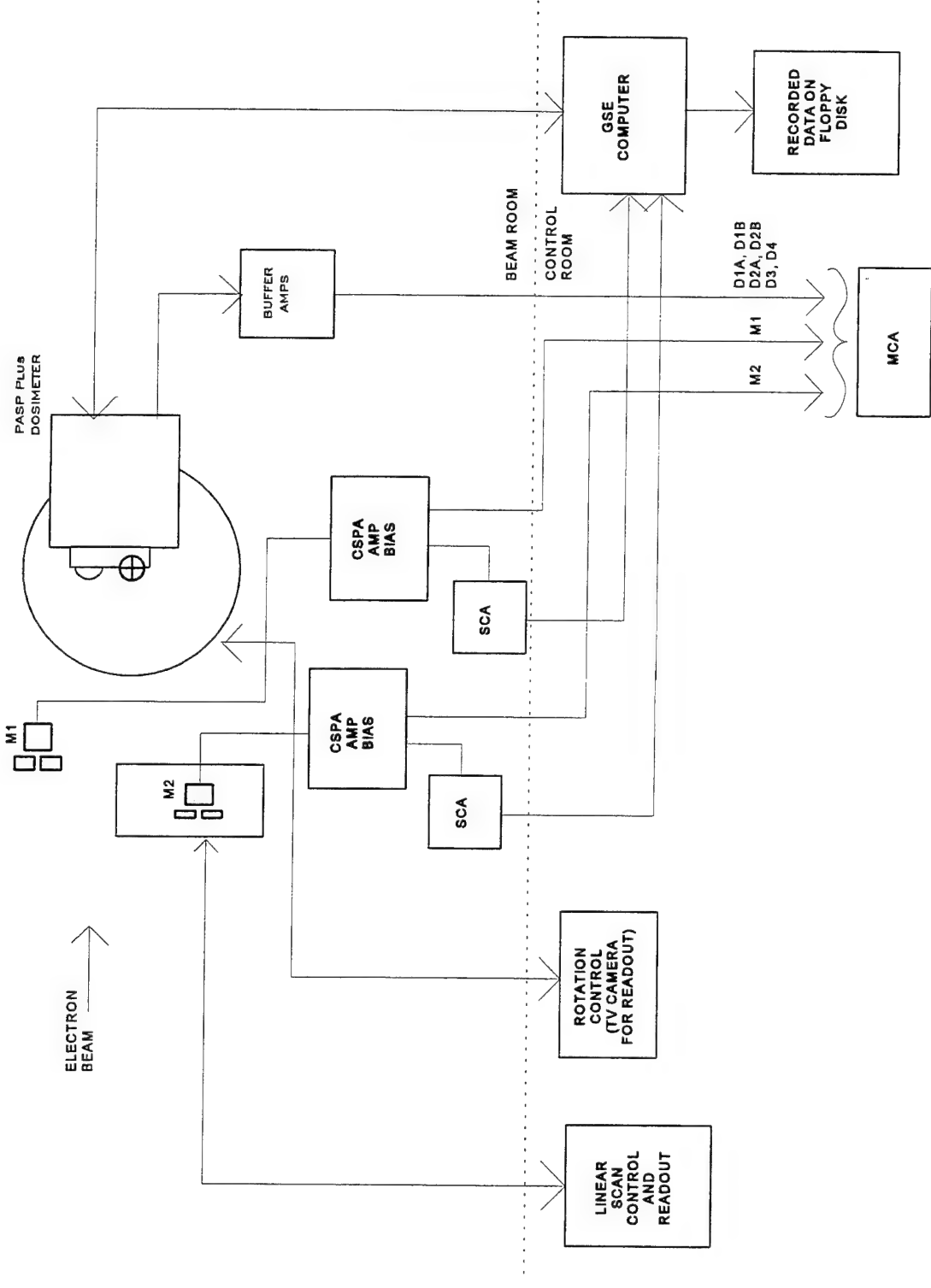


Figure 4. Electronics and Control Configuration for Electron Calibration at the MIT Van de Graaff.

were placed at the sides and in front of the dosimeter, a correction had to be made for the electron beam intensity distribution in both distance and angle. The corrections were derived from across-beam scans made with M2, where M2 was positioned just in front of the dosimeter. The electronics configuration is shown in Figure 4, with control of the dosimeter rotations and M2 scans, and data recording all being done outside the beam room. Dosimeter data and the M1 and M2 SCA (Single Channel Analyzer - integral threshold above 100 keV) counts were recorded simultaneously to avoid problems from beam intensity variations. Detector spectra (M1, M2, and Di, the dome detector being calibrated) were taken periodically during the calibration to provide beam monitoring and energy measurement, as well as to provide data on the electron energy loss spectra in the various detectors.

The Van de Graaff energy was set by using the reading of a digital panel meter on the control console. The beam energy in MeV is nominally twice the reading of the panel meter. The nominal electron beam energy was calibrated using the full-energy loss peaks in M1 and M2. Since M2 was 1500 microns thick (Figure 3) it gave a discernable full-energy peak even for the nominal 3.4 MeV beam. The internal (vacuum) electron energy is degraded by energy loss in the 3-mil thick Al vacuum window after the 90° analyzing magnet, and by the various air paths to M1 (d1), M2 (d2), and the dosimeter (df) (M2 also has a 0.3-mil thick Al light shield). The Dosimeter SN/1 electron calibrations were made during a single series of runs that involved only repositioning the dosimeter to get the different domes into the beam center.

Table 6 summarizes the run sets made, along with the detector distances shown in Figure 3. The Dosimeter SN/1 data file names listed are for the data recorded by the GSE computer. The monitor detector counts were recorded by the GSE for the same time period of Dosimeter count accumulation. Since the six detectors are cycled through once in every six readouts, six monitor counts must be summed to give the count corresponding to a given dosimeter detector count.

Table 6: Summary of PASP Plus Dosimeter SN/1 Calibration Run Sets

Dosimeter SN/1 Data File	Air path (inches) to front of			Type of Data taken
	M1 (d1)	M2 (d2)	Dosimeter	
92092203.*	20.75	20.25	25.00	D1 angle scan
92092303.*	20.75	20.25	25.00	D1 angle scan
92092305.*	20.75	20.25	25.00	D1 angle scan
92092401.*	20.75	20.25	25.00	D2 angle scan
92092500.*	20.75	20.25	25.00	D3 angle scan

The electron beam energy calibration was made from the M2 MCA (Multi Channel Analyzer) data taken during the different energy runs. The M2 gain was calibrated with the 477.3 keV Compton edge from the 661.6 keV gamma rays from a weak Cs-137 source. The MCA linearity and zero pulse height channel were measured using a precision Research Pulser. The M2 full energy loss peak energy for the electrons has to be corrected for the energy loss in the Al foils and the air path. The results are given in the first five columns of Table 7, for all of the energies used (Tr-Nom is the difference between the true electron energy in vacuum and the nominal value). Energy losses for the electrons were calculated using the tables for aluminum and air in Reference 4. The data from columns 1 and 5 in Table 7 are plotted in Figure 5, and have a best-fit straight line of

$$(\text{True} - \text{Nominal}) = -0.0869 \times \text{Nominal} + 0.1425 \quad (3.1)$$

The last two columns in Table 7 give the best fit results for the true electron energy in vacuum, and the effective electron energy for the Dosimeter SN/1 at the 25 inch position.

Table 7: Electron Energy Calibration for Dosimeter SN/1 Calibration

Nominal (MeV)	M2 Meas (MeV)	Total E Loss (MeV)		Meas Tr-Nom E (MeV)	Best Fit True Energy (MeV)	
		To M2	To Di		In Vac	At Di
0.25	0.169	0.186	0.202	0.105	0.371	0.169
0.30	0.237	0.174	0.191	0.111	0.416	0.225
0.40	0.345	0.159	0.180	0.104	0.508	0.328
0.50	0.444	0.150	0.171	0.094	0.599	0.428
0.75	0.690	0.142	0.162	0.082	0.827	0.665
1.00	0.922	0.140	0.160	0.062	1.056	0.896
1.25	1.150	0.139	0.159	0.039	1.284	1.125
1.50	1.373	0.140	0.160	0.013	1.512	1.352
1.75	1.608	0.141	0.161	-0.001	1.740	1.579
2.00	1.834	0.142	0.162	-0.024	1.969	1.807
2.25	2.074	0.144	0.164	-0.032	2.197	2.033
2.50	2.286	0.145	0.165	-0.069	2.425	2.260
2.75	2.509	0.146	0.167	-0.095	2.654	2.487
3.00	2.730	0.149	0.169	-0.121	2.882	2.713
3.25	2.954	0.159	0.170	-0.146	3.110	2.940
3.40	3.075	0.150	0.171	-0.175	3.247	3.076

The electron beam intensity profile was obtained from the M2 across-beam scans for all of the energies used. The electrons scatter in the 3 mil Al vacuum window and in the air path to the detectors. The beam intensity variation with distance is  $1/d^2$ , with  $d$  ( $d_1$ ,  $d_2$ , or  $d_f$ ) being the distance from the vacuum window to the detector in question. The profile across the beam is centered on the beam axis (Dosimeter dome center), and varies with energy. For all of the calibration data the M2 monitor was  $4 \frac{3}{4}$  inches in front of and  $2 \frac{1}{2}$  inches to the side of the Dosimeter dome being calibrated. Normalization corrections for M1 and M2 were made from M2 across-beam scan data using data taken at the normal M2 measurement position, and also using data taken with M2 directly in front of the Dosimeter dome.

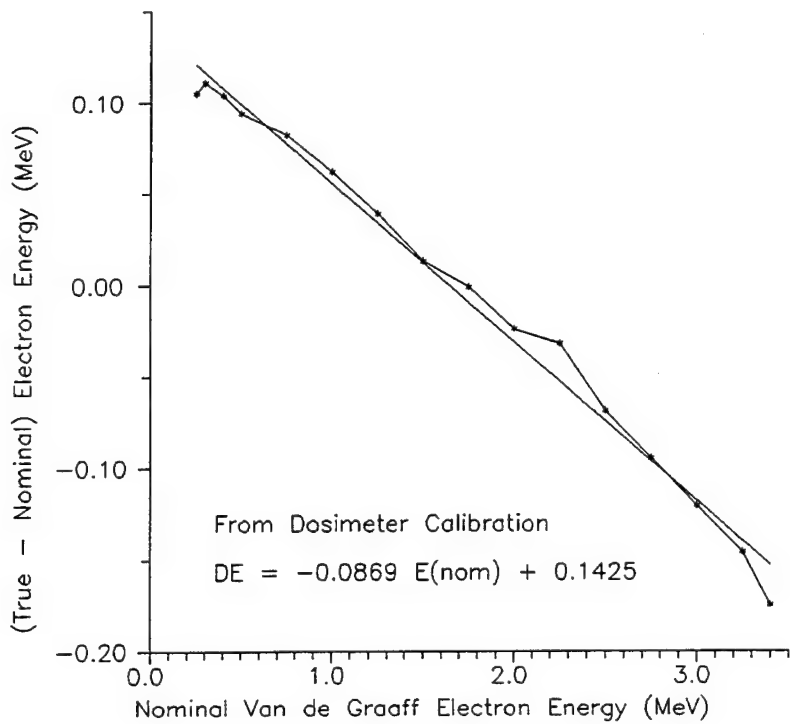


Figure 5. Electron Energy Calibration of the MIT Van de Graaff.

The Dosimeter detector counts measured for a given angle  $\theta$  were converted to a calibrated area from both the M1 and M2 counts by:

$$A_1(\text{cnt}) = \text{cnt}(D_i) \times A(M1) \times M_{1\text{fac}}/\text{cnt}(M1) \quad \text{cm}^2 \quad (3.2)$$

$$A_2(\text{cnt}) = \text{cnt}(D_i) \times A(M2) \times M_{2\text{fac}}/\text{cnt}(M2) \quad \text{cm}^2 \quad (3.3)$$

with the average value calculated as

$$A_{avg}(\theta) = (A_1(cnt) + A_2(cnt))/2 \text{ cm}^2. \quad (3.4)$$

In the above

$$M_{1fac} = (df/dl)^2 \times \frac{cnt(M1, M2 \text{ centered}) \times A(M2)}{cnt(M2, M2 \text{ centered}) \times A(M1)} \quad (3.5)$$

and

$$M_{2fac} = (df/dl)^2 \times \frac{cnt(M2) \times cnt(M1, M2 \text{ centered})}{cnt(M2, M2 \text{ centered}) \times cnt(M1)} \quad (3.6)$$

The symbols are

$cnt(Di)$  = sum of Dosimeter channel counts (D1A, D1B, etc.)

$A(M1)$  = 1.267  $\text{cm}^2$  is the collimated area of M1

$A(M2)$  = 0.173  $\text{cm}^2$  is the collimated area of M2

$cnt(M1)$  = M1 monitor count summed for the  $cnt(Di)$  period

$cnt(M2)$  = M2 monitor count summed for the  $cnt(Di)$  period

$cnt(M1, M2 \text{ centered})$  = M1 count when M2 is centered on the beam

$cnt(M2, M2 \text{ centered})$  = M2 count when M2 is centered on the beam

The normalization factors  $M_{1fac}$  and  $M_{2fac}$  use the results of the M2 across-beam scan and the  $1/d^2$  correction to provide the calibrated areas of Eqs. (3.2) and (3.3). This method allows direct correction for the measured beam profile for each calibration set, and reduces variations from slight beam changes from one calibration set to the next. The two measured areas are averaged to provide the final result for  $A_{avg}(\theta)$  in Eq. (3.4).

The dosimeter channel geometric factors were calculated from the measured  $A_{avg}(\theta)$  values by:

$$Gf = \sum A_{avg}(\theta_i) \Omega(\theta_i) \text{ cm}^2 \text{ sr}, \quad (3.7)$$

where

$$\Omega(\theta_i) = 2\pi (\cos(\theta_i - \Delta\theta_{i-}/2) - \cos(\theta_i + \Delta\theta_{i+}/2)) \text{ sr} \quad (3.8)$$

with  $\Delta\theta_{i-} = \theta_i - \theta_{i-1}$ ,  $\Delta\theta_{i+} = \theta_{i+1} - \theta_i$ . Note that for  $i = 1$ ,  $\Delta\theta_{i-} = 0$ , and for  $i = \max$ ,  $\Delta\theta_{i+} = \Delta\theta_{i-}$ . Measurements were generally made at  $0^\circ$ ,  $\pm 20^\circ$ ,  $\pm 40^\circ$ ,  $+60^\circ$ ,  $+80^\circ$ , and  $+90^\circ$ , with a repeat measurement at  $0^\circ$  to verify beam stability. The M2 across-beam scan was generally made after the dosimeter angular scan.

### 3.2 Calibrated Electron Response

The calibration results for the Dosimeter SN/1 D1 dome, channels D1A and D1B, are given in Table 8, and plotted in Figures 6 and 7. The data have not had the calibration source background counts subtracted since they are a small fraction of the measured counts for the D1A and D1B calibrations. The nominal Gf fits using Eq. (2.1) with the nominal SSD  $0^\circ$  areas are also plotted in Figures 6 and 7. The Gf fits using the nominal areas give a reasonable fit

Table 8: Dosimeter SN/1 D1A and D1B Calibrated Electron Responses

Electron Beam Energy (MeV)		D1A Calibration		D1B Calibration	
VdG Nom	Cal/Eff	Area(0°) ( $10^{-2}$ cm $^2$ )	G Factor ( $10^{-2}$ cm $^2$ sr)	Area(0°) ( $10^{-2}$ cm $^2$ )	G Factor ( $10^{-2}$ cm $^2$ sr)
0.25	0.169	0.0103	0.0231	0.0489	0.138
0.30	0.225	0.346	0.861	2.36	5.65
0.40	0.328	1.253	3.05	7.64	18.87
0.50	0.428	1.486	3.88	8.81	22.19
0.75	0.665	1.675	4.30	8.64	17.95
1.00	0.896	1.567	4.42	8.19	20.37
1.25	1.125	1.588	4.39	8.24	19.69
1.50	1.352	1.476	4.33	8.02	19.16
1.75	1.579	1.362	4.24	7.61	18.72
2.00	1.807	1.345	4.39	7.54	19.07
2.50	2.260	1.482	4.90	7.04	18.50

Table 9: Dosimeter SN/1 D2A and D2B Calibrated Electron Responses

Electron Beam Energy (MeV)		D2A Calibration		D2B Calibration	
VdG Nom	Cal/Eff	Area(0°) ( $10^{-2}$ cm $^2$ )	G Factor ( $10^{-2}$ cm $^2$ sr)	Area(0°) ( $10^{-2}$ cm $^2$ )	G Factor ( $10^{-2}$ cm $^2$ sr)
1.25	1.125	0.00169	0.00925	0.0153	0.0645
1.50	1.352	0.0478	0.1642	0.2622	1.059
1.75	1.579	0.1506	0.635	0.837	3.57
2.00	1.807	0.2832	1.193	1.535	6.71
2.25	2.033	0.419	1.710	2.209	9.22
2.50	2.260	0.561	2.314	2.912	11.90
2.75	2.487	0.702	3.01	3.60	14.44
3.00	2.713	0.963	4.16	4.29	17.61
3.25	2.940	1.552	6.26	5.39	22.30

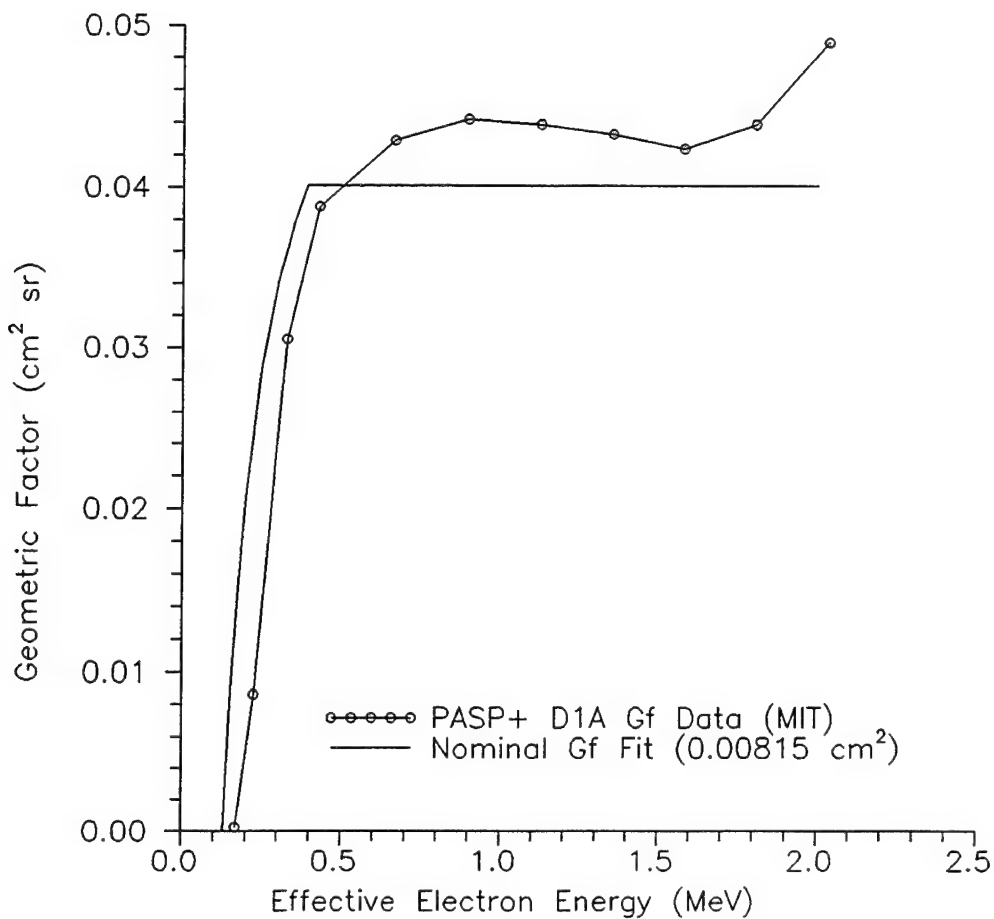


Figure 6. Dosimeter SN/1 D1A Calibrated Electron Geometric Factors.

to the high energy Gf values, but the effective threshold energy from the calibration data is somewhat higher. The energy at which the Gf value is half of the high energy limit is about 0.27 MeV for the calibration data, but the nominal Gf fit gives 0.195 MeV.

The calibration results for the Dosimeter SN/1 D2 dome, channels D2A and D2B, are given in Table 9, and plotted in Figures 8 and 9. The D2A channel is identical to the D1 channel of the CRRES dosimeter (Reference 3), so the CRRES D1 calibration data and Gf fit are also plotted in Figure 8. The CRRES D1 Gf fit required a value  $A_{no} = 0.01744 \text{ cm}^2$ , which is about twice the nominal area of  $0.00815 \text{ cm}^2$ . This is an effect of the scattering of the electrons in the SSD, as discussed in Reference 3. The effective value of  $A_{no}$  is better given as:

$$\begin{aligned}
 A_{no,eff} &= A_{no} + \pi \times d \times t \\
 &= 0.00815 + \pi \times 0.1019 \times 0.04 \\
 &= 0.0210 \text{ cm}^2
 \end{aligned} \tag{3.9}$$

where  $A_{no}$  is the area of the sensitive volume of the detector (Table 1),  $d$  is the diameter of  $A_{no}$ , and  $t$  is the detector thickness. This effect is largest for the smallest area SSDs, where the diameter  $d$  is only a few times the thickness  $t$ .

The D2B Gf data in Figure 9 are compared with the Gf fit of Eq. (2.1) using a nominal value of  $A_{no} = 0.0514 \text{ cm}^2$ . Using Eq. (3.9) gives  $A_{no,\text{eff}} = 0.0835 \text{ cm}^2$ , which would raise the Gf fit curve by a factor of 1.6. Since the MIT Van de Graaff limits near 3.5 MeV, the high energy limit of Gf for the PASP Plus dosimeter D2 dome was barely reached. An estimate of the energy at which the D2 dome Gf value is half of the high energy limit is about 2.1 MeV for the calibration data, but the nominal Gf fit gives 1.50 MeV. The measured Gf half-height energies are about 1.4 times the nominal fit Gf half-height energies, for both the D1 and D2 domes.

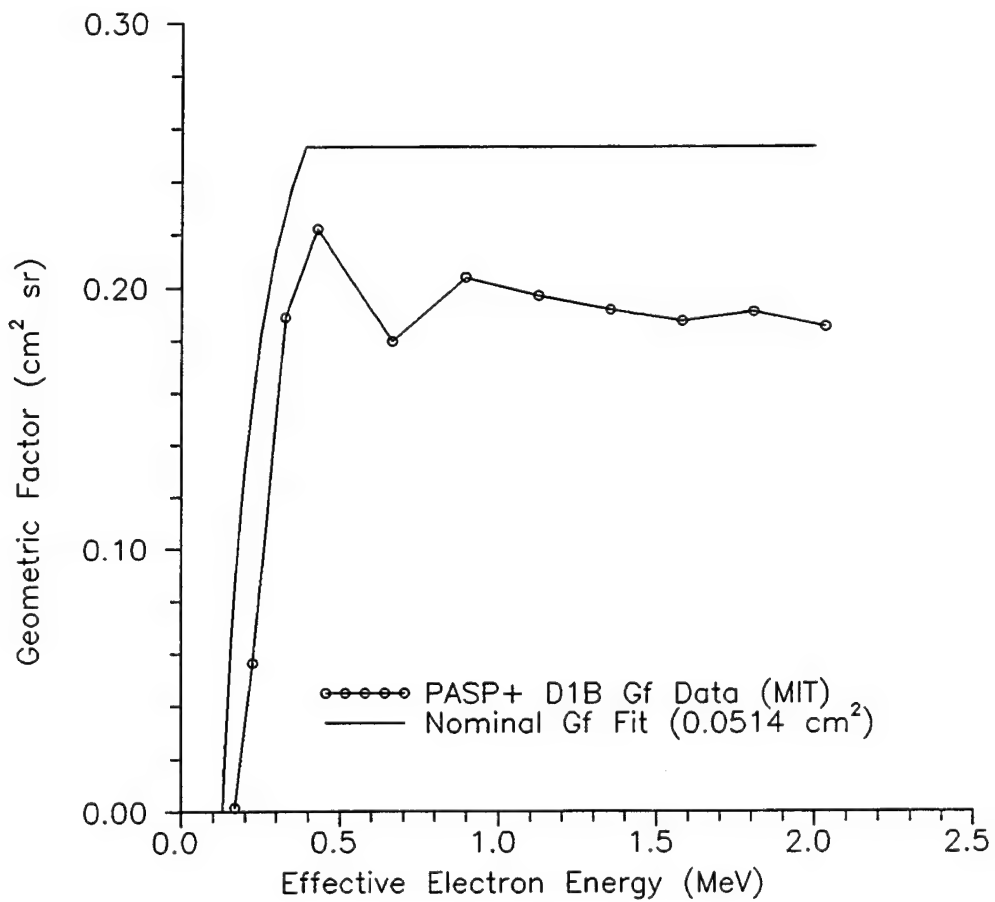


Figure 7. Dosimeter SN/1 D1B Calibrated Electron Geometric Factors.

The calibration results for the Dosimeter SN/1 D3 dome/channel are given in Table 10, and plotted in Figure 10. The D3 channel is

identical to the D2 channel of the CRRES dosimeter (Reference 3), so the CRRES D2 calibration data and nominal Gf fit are also plotted in Figure 10. The CRRES D2 Gf fit required a value  $A_{no} = 0.075 \text{ cm}^2$  (Reference 3), while Eq. (3.9) gives  $A_{no,eff} = 0.0835 \text{ cm}^2$ , which is reasonable agreement. The PASP Plus dosimeter D3 calibration data only show the very beginning of the rise in Gf, but it appears to be in reasonable agreement with the CRRES D2 Gf calibration data. The measured CRRES D2 Gf half-height energy is about 4.5 MeV, about 1.2 times the nominal Gf fit half-height energy of 3.75 MeV.

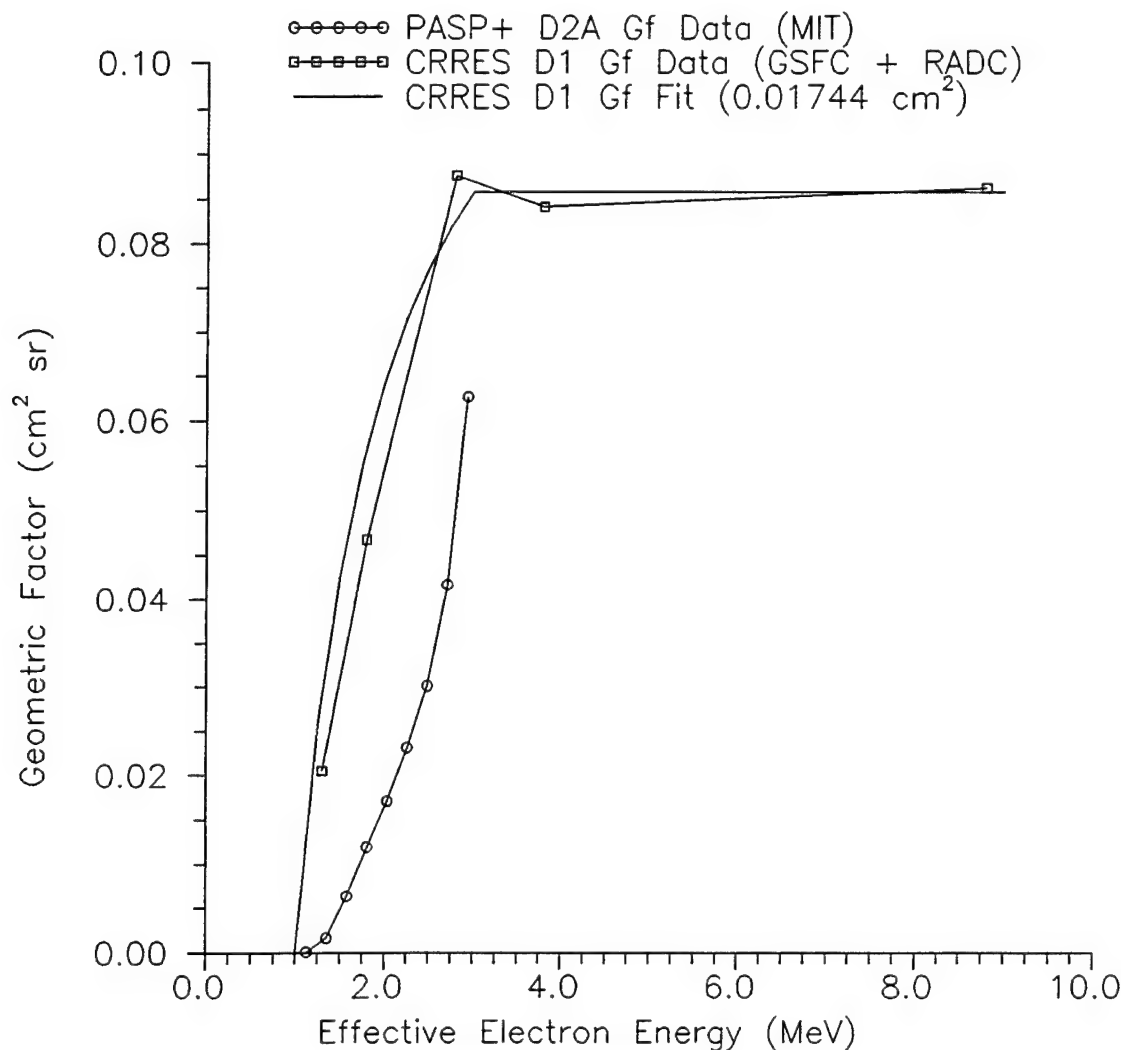


Figure 8. Dosimeter SN/1 D2A Calibrated Electron Geometric Factors.

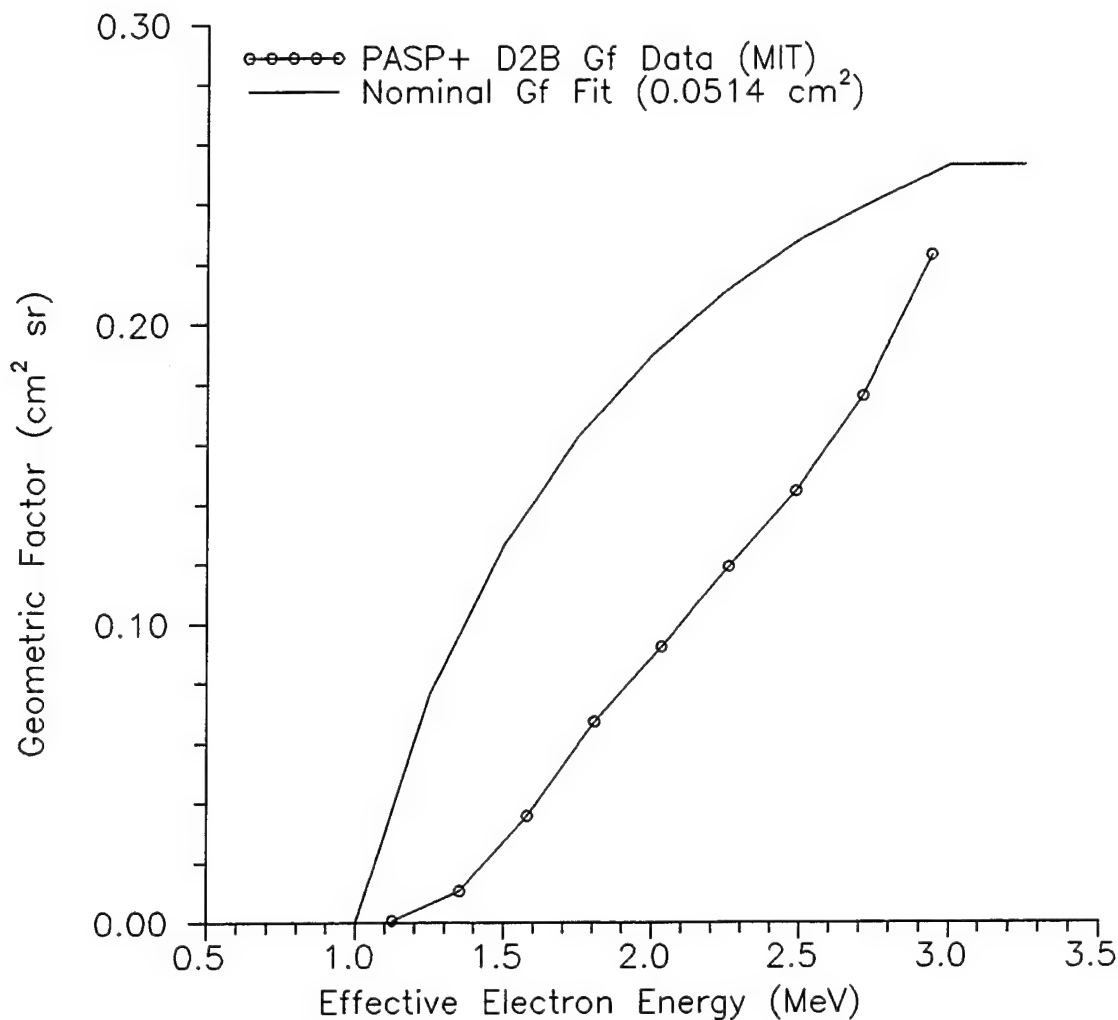


Figure 9. Dosimeter SN/1 D2B Calibrated Electron Geometric Factors.

The dosimeter electron response fit in Eq. (2.1) was generated from the DMSP/F7 dosimeter calibration data (Reference 2), which was most reliable for the highest energies (above about 4 MeV). The CRRES dosimeter was calibrated at lower electron energies at both the NASA/GSFC Van de Graaff, and at the RADC Linear Accelerator (Linac; Reference 3). The GSFC calibrations covered only the electron energies below about 1.8 MeV, and provided only a comparatively small area electron beam (about 0.25 inch diameter). Also, the GSFC beam monitor measured intensity only before and after each dosimeter measurement, and there is some question of the beam energy calibration.

The low-energy electron calibration of the CRRES dosimeter at the RADC Linac suffered from a weak beam intensity and a large

Table 10: Dosimeter SN/1 D3 Calibrated Electron Responses

Electron Beam Energy (MeV)		D3 Calibration	
VdG Nom	Cal/Eff	Area ( $0^\circ$ ) ( $10^{-4} \text{ cm}^2$ )	G Factor ( $10^{-4} \text{ cm}^2\text{sr}$ )
2.50	2.260	0.372	2.94
2.75	2.487	0.517	5.38
3.00	2.713	1.353	12.86
3.25	2.940	8.12	46.5
3.40	3.076	13.90	96.9

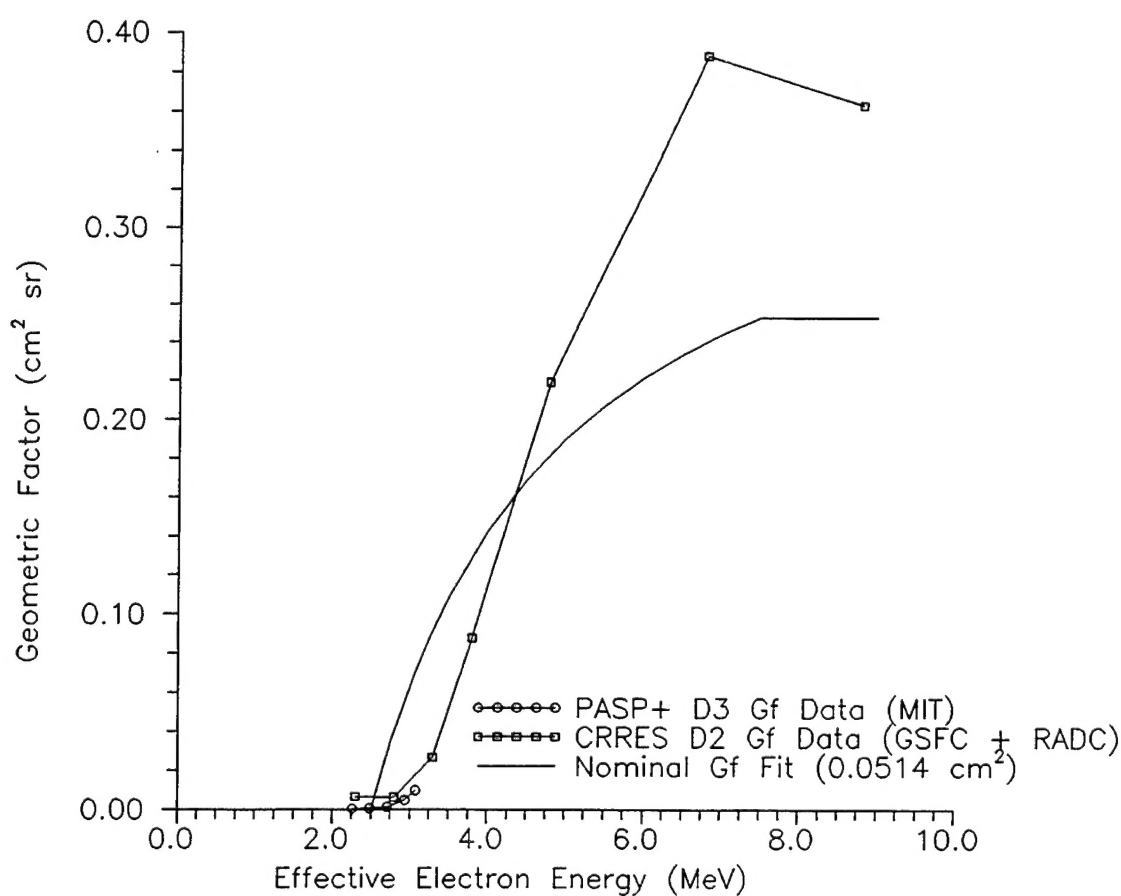


Figure 10. Dosimeter SN/1 D3 Calibrated Electron Geometric Factors.

energy spread in the beam. The lowest energy channel electron response, i.e. the D1 dome on the CRRES and DMSP/F7 dosimeters, is thus somewhat uncertain, and it is felt that the detailed calibration measurements made with the PASP Plus dosimeter at the MIT Van de Graaff are the more accurate. The PASP Plus dosimeter shows about a 40% difference between the measured and fit half-height response energies for both the D1 (0.15 MeV electron threshold) and the D2 (1.0 MeV electron threshold) channels, which decreases to 20% for the D3 (2.5 MeV electron threshold) channel. The fit of eq.(2.1) should be quite good for the highest energy D4 (5.0 MeV electron threshold) channel.

The measured angular responses of the PASP Plus dosimeter are summarized by the plots in Figures 11 and 12. Figure 11 shows the angular response of the D1B channel for electrons of 0.328, 1.125 and 2.037 MeV energy. A  $\cos(\theta)$  curve is also plotted, and shows reasonable agreement up to at least  $60^\circ$ . Use of a full  $\cos(\theta)$  fit out to  $90^\circ$  gives a reasonable approximation for the full Gf value. The measured angular response is in reasonable agreement with that expected for the flat shield of the D1 dome.

The D2B channel angular responses for electrons of 1.579, 2.260 and 2.940 MeV energy are shown in Figure 12. The plotted fit is for

$$(A_n(\theta)/A_n(0))_{\text{fit}} = (2 + 3 \times \cos(\theta))/5 \quad (3.10)$$

which was found for the earlier dosimeter dome calibrations (References 2, 3), and provides a reasonable fit to the new measurements. The D3 and D4 domes are expected to have similar electron angular responses.

#### 4. Summary and Conclusions

Two dosimeters have been fabricated for use on the APEX satellite, with the dosimeter SN/2 being presently installed as part of the PASP Plus payload. The launch of the APEX spacecraft took place on 3 August 1994. The PASP Plus dosimeter provides six (6) channels for dose measurement under four (4) thicknesses of aluminum shielding. The two thinnest aluminum shields have two detectors of different sizes to allow for a larger dynamic range in particle flux. The nominal electron threshold energies of the four domes (range-energy table calculations) are 0.15 MeV, 1.0 MeV, 2.5 MeV and 5.0 MeV.

The dosimeter SN/1 was calibrated with electrons at an MIT Van de Graaff accelerator. Measurements were made with effective electron energies of 0.169 MeV to 3.076 MeV. The low energy data are in disagreement with earlier calibration data for the CRRES and DMSP/F7 dosimeters, but the newer electron calibration data are believed to be the more accurate. The previous electron calibration data are more accurate at the higher ( $>4$  MeV) energies, and the newer calibration data are in better agreement at the high-energy end.

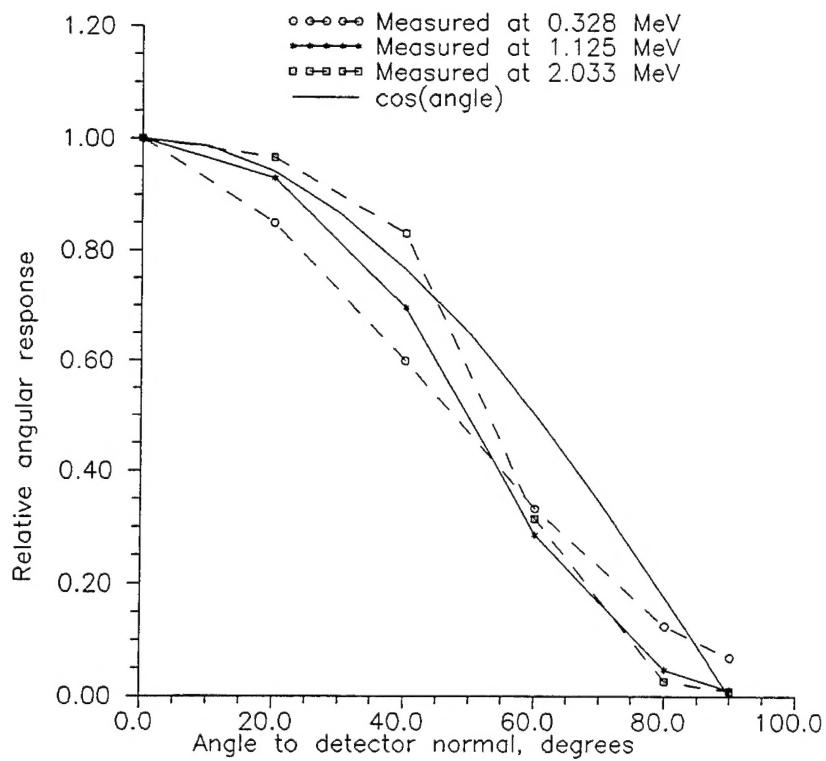


Figure 11. Measured Angular Response of D1B for Electrons.

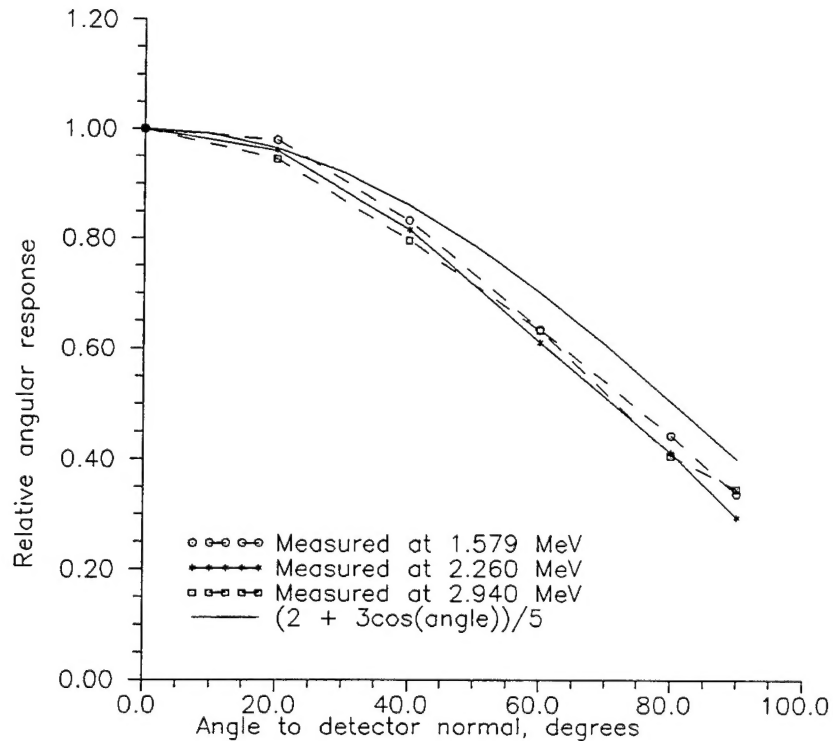


Figure 12. Measured Angular Response of D2B for Electrons.

## References

1. P. R. Morel, F. Hanser, J. Belue and R. Cohen, "Develop and Fabricate a Radiation Dose Measurement System for Satellites", Report PL-TR-94-2277 (November 1994), ADA295137.
2. M. S. Gussenhoven, E. G. Mullen, R. C. Filz, F. A. Hanser and K. A. Lynch, "Space Radiation Dosimeter SSJ\* for the Block 5D/Flight 7 DMSP Satellite: Calibration and Data Presentation", Report AFGL-TR-86-0065 (20 March 1986), ADA172178.
3. B. K. Dichter and F. A. Hanser, "Development and Use of Data Analysis Procedures for the CRRES Payloads AFGL-701-2/Dosimeter and AFGL-701-4/Fluxmeter and Application of the Data Analysis Results to Improve the Static and Dynamic Models of the Earth's Radiation Belts", Report PL-TR-92-2066 (March 1992), ADA253287.
4. M. J. Berger and S. M. Seltzer, "Tables of Energy Losses and Ranges of Electrons and Positrons", NASA SP-3012 (1964).